Journal of The Electrochemical Society

OPEN ACCESS

$Li_{15}Si_4$ Formation in Silicon Thin Film Negative Electrodes

$Li_{15}Si_4$ Formation in Silicon Thin Film Negative Electrodes

D. S. M. Iaboni and M. N. Obrovac[*,z]

Department of Chemistry, Dalhousie University, Halifax, Nova Scotia B3H 4R2, Canada

The conditions for $Li_{15}Si_4$ formation in Si thin film negative electrodes was studied during charge and discharge cycling in lithium cells. It was found that $Li_{15}Si_4$ formation can be suppressed during cycling of Si thin films by stress induced from the presence of the substrate. Furthermore, $Li_{15}Si_4$ formation was found to be coincidental with capacity fade and delamination of the Si film from the current collector. These results deepen the understanding of the cycling of Si thin films. Moreover, they have profound implications for Si alloy negative electrodes for Li-ion batteries, as the presence of $Li_{15}Si_4$ during cycling can be used as a sensitive indicator for weakly bound Si regions.

 [DOI: 10.1149/2.0551602jes]

Manuscript submitted September 25, 2015; revised manuscript received November 3, 2015. Published November 19, 2015.

The development of Li-ion batteries that incorporate energy dense silicon-based negative electrodes is challenging, mainly because of silicon's volume expansion upon lithiation. Furthermore, crystalline $Li_{15}Si_4$ has been shown to form during the lithiation of silicon when the voltage becomes less than 50 mV.[1] Acoustic emission studies and imaging techniques have indicated that this phase transition can result in high internal stresses, leading to particle fracture and cell fade.[2] To overcome the issues associated with $Li_{15}Si_4$ phase formation and volume expansion during cycling, researchers have demonstrated high cycle life in Li cells by using Si in the form of nanoparticles,[3,4] nanowires,[5,6] nanopillars,[7,8] thin films,[9,10] and in alloys with inactive or active phases.[11,12] These studies have reported various threshold sizes for nanoparticles (150 nm),[3,4] nanowires (300 nm),[13] and amorphous thin films (2.5 μm),[14] below which $Li_{15}Si_4$ formation does not occur. These results imply that the $Li_{15}Si_4$ phase may be a consequence of particle aggregation; however, the variance in threshold size among Si morphologies raises questions. In particular, the suppression of $Li_{15}Si_4$ formation in thin films that are microns thick is startling.

Recent studies have shown that the potential of Si electrodes can be significantly modified by applied stress.[15,16] Yang et al. have simulated the effect of a Cu layer bonded to one side of a Si anode on its electrochemistry and predict that it leads to asymmetric diffusion, resulting in stress fields that may limit Li-ion insertion into Si films.[17] Sethuraman et al. have made careful measurements of the effects of applied stress to Si thin films by measuring the substrate curvature changes during electrochemical lithiation and delithiation.[15] They determined the applied stress-potential coupling to be in the range of 100–125 mV/GPa for Si thin films. As the Si film expands during lithiation compressive stress results from its attachment to a fixed Cu substrate. This compressive stress was found to reach 1.5 GPa before being relieved by plastic flow. During delithiation, the Si film undergoes tensile stress as it contracts. This stress can be relieved by cracking. As a result the total electrode tensile stress during delithiation was found to be only 0.5 GPa, while the internal film stress during delithiation could not be measured by the methods used by Sethuraman et al., since the crack density was not known.[15] As a result of these studies, it was found that the voltage curve of silicon could be lowered by as much as 200 mV during lithiation. This causes Si electrodes to reach their lower cut off potential at an earlier state of charge, resulting in reduced capacity.

Since $Li_{15}Si_4$ has been shown to form at voltages between 50–70 mV, we note that the suppression of $Li_{15}Si_4$ formation in Si thin films observed by Hatchard et al.[14] can easily be accounted for within the magnitude of the lithiation voltage lowering observed from stress due to expansion against the substrate, as reported by Sethuraman et al. The conjecture that $Li_{15}Si_4$ formation in Si thin films can be suppressed by induced stress from a substrate is investigated here and implications for the cycling of Si-alloys in general are discussed.

Experimental

Samples were prepared by magnetron sputtering using a Corona Vacuum Coater's V3T system. Films were deposited using either one or two Si targets (Pure Tech, 99.9%) using a dc power supply of 150 W. The films were deposited onto cold-rolled Cu foil (CR-Cu), electrolytic Cu foil (E-Cu) (Furukawa Electric, Japan), and Ni foil (Special Metals Wiggin Ltd.). Some of the foils were roughened using Scotch-Brite (3M Company) prior to sputtering. These foils are designated with a superscript 'R', e.g. as CR-Cu^R (for cold-rolled Cu foil that was roughened). Si film mass was determined via position, using a calibration of the mass as a function of the sputtered film area with reference to pre-weighed Cu foil discs. A silicon wafer partially covered with Scotch tape (3M Company) was sputtered upon in each cycling run. The tape was subsequently removed and the sputtered wafer was then used to determine film thickness for each run using a Sloan DekTak profilometer. Film thickness ranged from 275 nm to 1200 nm. Scanning electron microscopy (SEM) was performed using a Phenom G2-pro SEM.

Sputtered Si film was removed from the copper substrate by dissolving the Cu in dilute HNO_3 (Caledon, 68.0% by weight) under a flow of Ar gas. The resulting amorphous Si flakes were recovered by suction filtration and washed with water. The washed product was incorporated into an electrode slurry composed of the recovered Si flakes, Super C Carbon Black (Timcal), and lithium polyacrylate (Li-PAA made by neutralizing polyacrylic acid (Aldrich) with $LiOH \cdot H_2O$ (Aldrich, ≥98% purity)) in a 20/32/48 weight ratio, respectively. The slurry was mixed by placing it in a 40 mL hardened stainless steel planetary mill vial containing two 1.27 cm tungsten carbide balls and mixing with a Retsch PM 200 planetary mill for 1 hour at 100 rpm. The slurry was then hand-coated onto electrolytic copper foil (Furukawa Electric, Japan) at a thickness of 0.10 mm using a stainless steel coating bar and dried at 120°C for 1 hour in air followed by 3 hours of drying at 120°C under vacuum. 1.26 cm^2 Cu discs were punched from the sputtered films or from the Si flake coatings and incorporated into 2325 coin cells with Li metal counter electrodes and 1 M $LiPF_6$ (BASF) in ethylene carbonate/diethyl carbonate/fluoroethylene carbonate (battery grade solvents from Novolyte) in a 3:6:1 v/v/v ratio electrolyte. Cells were cycled using a Maccor Series 4,000 Automated Test system at 30°C between 0.005 V and 0.9 V at a C/2 rate with a C/20 trickle current cutoff at 5 mV during discharge (lithiation), unless specified otherwise.

Results and Discussion

Figures 1a and 1b show the potential versus specific capacity plot and differential capacity curve, respectively, of a Li half-cell with a

*Electrochemical Society Active Member.
[z]E-mail: mobrovac@dal.ca

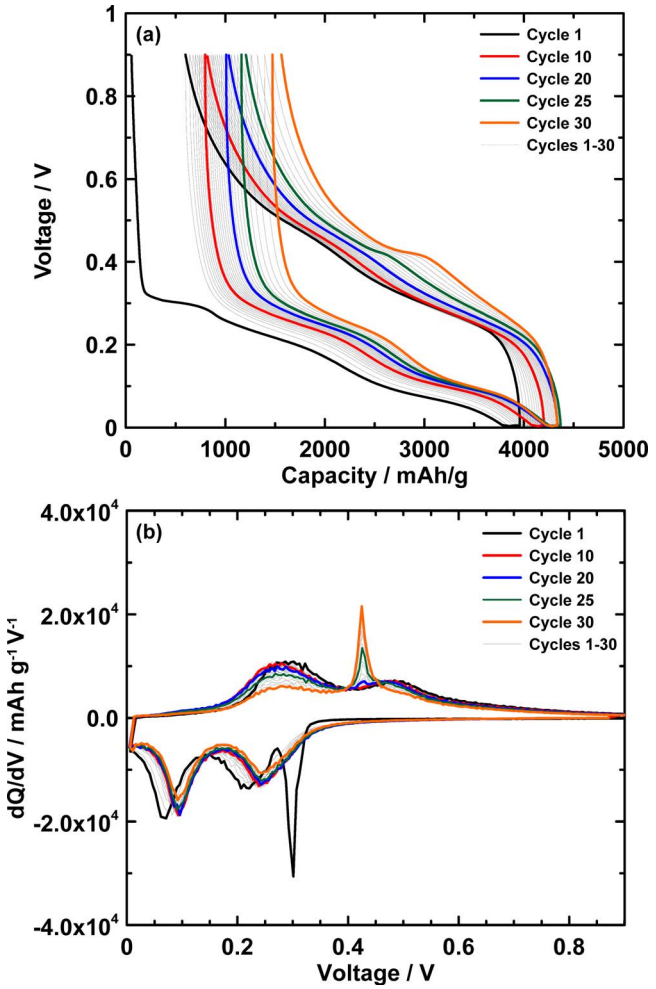

Figure 1. (a) Voltage versus capacity and (b) differential capacity curves of a 275 nm thick Si film sputtered onto CR-Cu cycling at a C/2 rate with a C/20 trickle. Cycles 1, 10, 20, 25, and 30 have been highlighted.

negative electrode comprised of a 275 nm Si thin film sputtered onto CR-Cu using one Si target, cycling at C/2 rate with a C/20 trickle. This film has a thickness well below the 2.5 μm threshold thickness

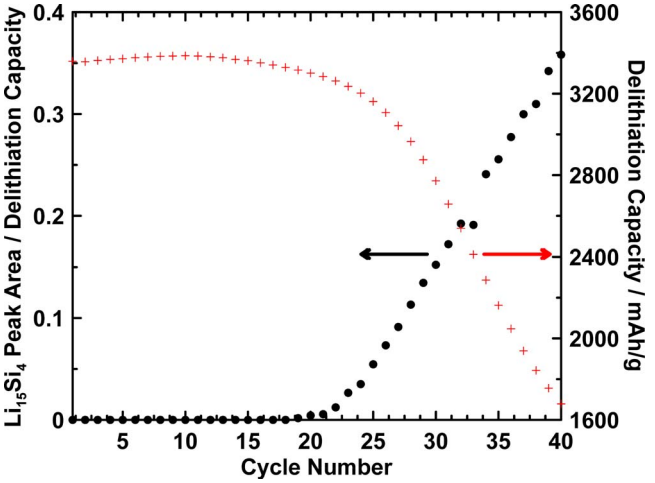

Figure 3. Relative $Li_{15}Si_4$ peak area, and delithiation capacity vs. cycle number for the same half-cell used in Figures 1 and 2.

reported by Hatchard et al., below which they reported $Li_{15}Si_4$ does not form after 10 cycles.[14] Initially the voltage curve in Figure 1a shows a small plateau at about 0.25 V (likely due to nucleation processes during initial lithiation). The voltage and differential capacity curves are then characteristic of amorphous Si for the first 20 cycles; however, there appears to be a significant shift to higher voltage in the lithiation differential capacity profile (about 20 mV) between cycle 1 and cycle 10. To our knowledge, this phenomenon has not been previously reported. At cycle 20 a small peak in the delithiation differential capacity appears near 0.42 V, which corresponds to the formation of $Li_{15}Si_4$. As cycling progresses, this peak increases in area during cycling, indicating a substantial increase in the formation of $Li_{15}Si_4$ during cycling. We believe that Hatchard et al. did not observe the formation of $Li_{15}Si_4$ in their thin films because not enough cycles were measured (Hatchard et al. only reported measuring 10 cycles[14]). As will be shown below, the composition and morphology of the substrate surface can also significantly affect when the $Li_{15}Si_4$ phase is observed.

Differential capacity delithiation curves were fit using a least squares minimization routine in order to quantify the degree of $Li_{15}Si_4$ formation during cycling, as shown in Figure 2. Three pseudo-Voigt peaks and a linear background were found to fit the entire delithiation profiles well. The peak fitting results are summarized in Figure 3,

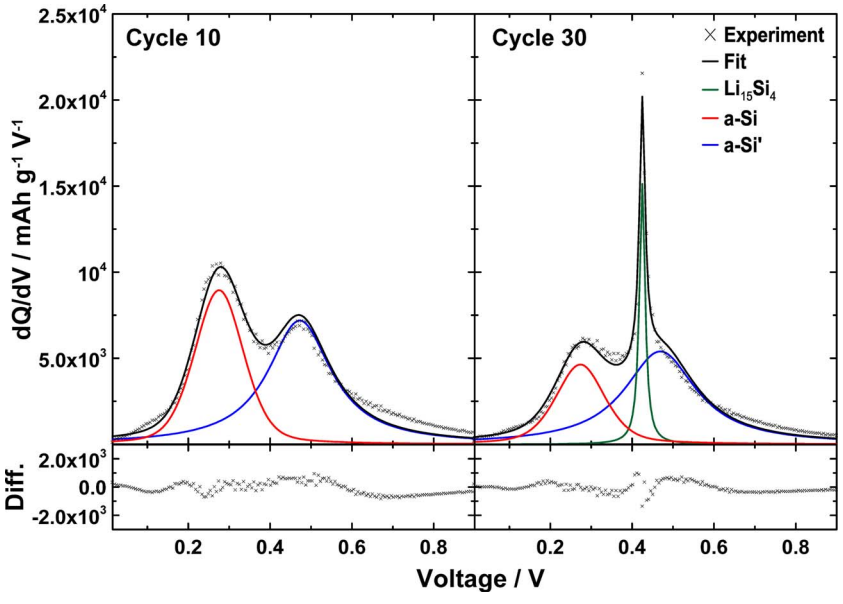

Figure 2. Differential capacity curve of (a) the 10th and (b) the 30th charge cycle for the same half-cell used in Figure 1. Also shown in these plots are the pseudo-Voight peak profiles used to fit the experimental data, the total calculated fit, and the difference between the fit and experiment.

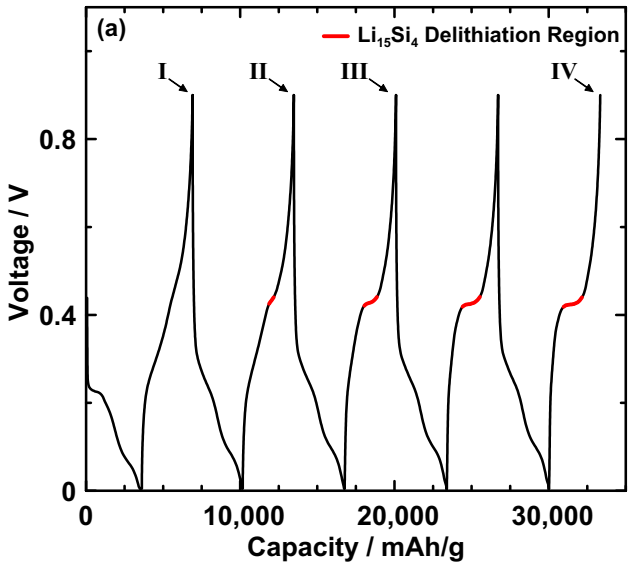

(b)

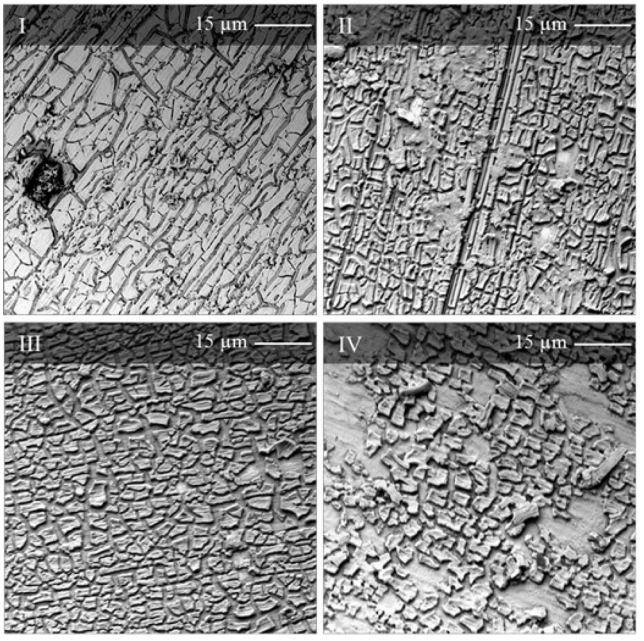

Figure 4. (a) Voltage versus capacity curve of a 450 nm thick Si film on E-Cu^R cycling at a C/4 rate with a C/20 trickle. Red lines indicate the growing $Li_{15}Si_4$ delithiation region. Roman numerals indicate points where cells were disassembled for SEM imaging. (b) I - IV are the resulting SEM images at each of the indicated points in (a).

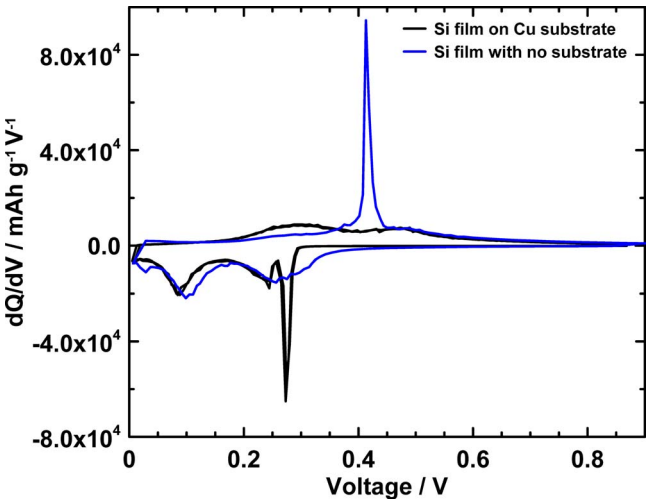

Figure 5. Differential capacity curve for the first cycle of a 450 nm Si film sputtered onto a E-Cu^R (in black) and one of a Si composite coating where the Si was obtained by dissolving the Cu substrate of a Si thin film in HNO_3 and recovering the Si flakes.

which shows the total delithiation capacity and the relative amount of delithiation capacity from $Li_{15}Si_4$ for the same film shown in Figure 1. In this example, no $Li_{15}Si_4$ is present in early cycling; however, after cycle 20 significant amounts of $Li_{15}Si_4$ progressively form. Furthermore, significant capacity fade is coincident with $Li_{15}Si_4$ formation.

In order to understand the physical basis for the observed $Li_{15}Si_4$ formation and coincident fade during cycling, fully delithiated electrodes were examined by SEM as a function of cycle number. Figure 4a shows the voltage curve of a 450 nm thick Si film sputtered on E-Cu^R. This film forms $Li_{15}Si_4$ early on in cycling. The extent of $Li_{15}Si_4$ can be visualized as the length of the $Li_{15}Si_4$ plateau, which is highlighted in the figure. Figure 4b shows SEM images of this film after cycling 1, 2, 3 and 5 cycles (as indicated by roman numerals in Figure 4a). All films were in their fully delithiated state. After the first cycle (Figure 4bI), there is widespread cracking and trench formation, resulting in the formation of Si islands; however, the film has not disconnected from the substrate and appears to be lying flat in the SEM image. At this stage no $Li_{15}Si_4$ can be detected in the voltage curve. The flatness of the islands can be visualized in Figure 4b as the islands appear perfectly homogeneous in their shading throughout the image. After cycle 2 (Figure 4bII), some of the edges of the Si islands have disconnected from the substrate (as shown by the inhomogeneous shading at the edges of the islands in the SEM image) and a small amount of $Li_{15}Si_4$ can be detected in the voltage curve. After cycle 3 (Figure 4bIII), there is significant delamination of the film from the substrate. This delamination is coincident with significant $Li_{15}Si_4$ capacity in the voltage curve. After cycle 5 (Figure 4bIV), Si islands are only attached to the substrate by small point contacts and most of them are so weakly bound that they detach entirely upon cell disassembly. Coincidentally, the $Li_{15}Si_4$ plateau now accounts for nearly the entire delithiation capacity for this cycle.

These results strongly imply a relationship between film delamination and increased $Li_{15}Si_4$ formation. To confirm this relationship, a portion of a 450 nm Si film sputtered on E-Cu^R was cycled as is, while the Si film from another portion of the electrode was removed from its substrate by dissolving the Cu substrate in nitric acid. The recovered Si film flakes were then incorporated into a composite coating. Figure 5 shows the differential capacity curve of the first cycle of the composite coating and that of the original Si film attached to the E-Cu^R substrate. There is significant $Li_{15}Si_4$ formation in the Si film with no substrate. In contrast, the original Si film attached to the Cu foil shows no sign of $Li_{15}Si_4$ formation. In addition, the peak at about 0.08 V during delithiation is at a much lower potential for the Si film bonded to the E-Cu^R substrate than the Si film with no substrate. This shift is consistent with voltage depression caused by compressive stress. The results shown in Figures 3–5 imply that the suppression of $Li_{15}Si_4$ formation in sputtered films is entirely due to effects from the substrate and that $Li_{15}Si_4$ formation and fade are direct results of Si film delamination. This explains why 2 µm thick Si films sputtered on substrates were reported not to form $Li_{15}Si_4$ during cycling, while $Li_{15}Si_4$ forms during the cycling of much smaller Si particles (even nanoparticles).

Figure 6I–6VIII illustrates the process of $Li_{15}Si_4$ formation during the cycling of a Si thin film bonded to a substrate, and its relationship with capacity fade. When the pristine Si film (I) is first lithiated it can only expand in a direction perpendicular to the substrate. This

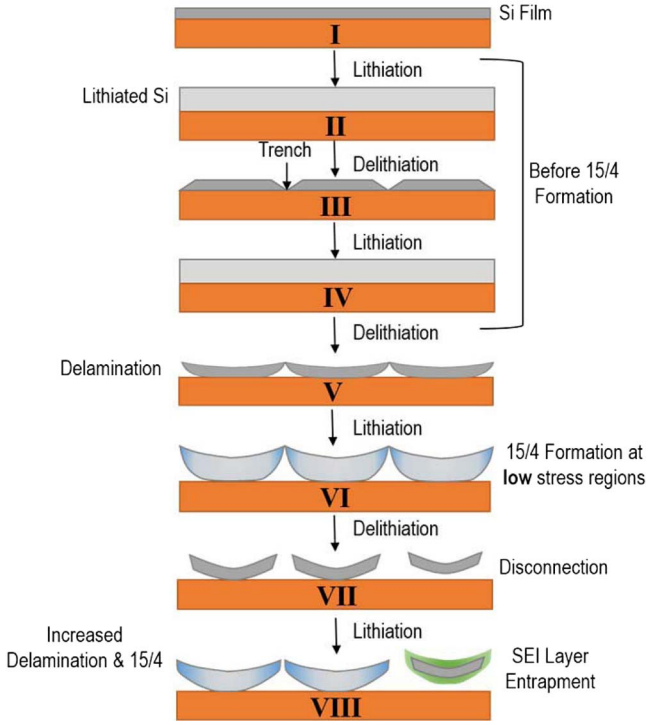

Figure 6. Illustration of the processes that occur during the cycling of a Si thin film, resulting in $Li_{15}Si_4$ formation, disconnection and fade.

causes large compressive stresses to form and the film undergoes plastic flow, increasing its thickness (II). Because of the large stresses that occur during this process, the voltage is depressed, by up to ~200 mV.[15,16] This causes the $Li_{15}Si_4$ formation voltage to be shifted below 0 V, and therefore this phase does not form at full lithiation. During delithiation, the film begins to contract. Large tensile stresses develop, causing the voltage to be elevated above the equilibrium voltage. Some of the tensile stress can be alleviated by crack formation, as shown in (III). Initially, as observed in Figure 4, the film remains bonded to the substrate and the cracks are in the form of trenches. During subsequent lithiations, the film expands, undergoing compressive stress and plastic flow. This expansion causes the cracks to close and the film to expand in thickness again (IV). Because the film is under compressive stress, $Li_{15}Si_4$ does not form, as explained above. These observations of Si film expansion and crack propagation have been observed previously.[18] After repetitive cycling, the Si thin film eventually begins to detach from the substrate (V). The detached regions now experience much less stress during lithiation, and, as a result, the voltage curve of Si in these regions is affected less by stress effects. Therefore, in these regions $Li_{15}Si_4$ forms at full lithiation (VI). During repeated cycling, the film becomes increasingly detached and more $Li_{15}Si_4$ forms at full lithiation. Eventually, Si islands detach entirely (VII). These islands likely then become completely surrounded by the solid electrolyte interphase and become electronically isolated (VIII), resulting in capacity fade.

The model proposed in Figure 6 implies that using different substrates that have different adhesion to the Si film may significantly affect electrochemical performance. To test this theory, a 275 nm film of Si was simultaneously sputtered onto various substrates, so that the sputtering conditions were identical for each substrate. Figure 7 shows the cycling performance of the resulting thin film electrodes. It can be seen that substrate composition and surface morphology both significantly impact the cycle life of a Si thin film. These effects can be rationalized in terms of the model proposed in Figure 6. For instance, Si sputtered onto CR-Cu had the worst cycling performance. Since the cold rolling process utilizes lubricants, one might expect that any lubricating oil layer on the Cu foil would cause the Si film adhesion

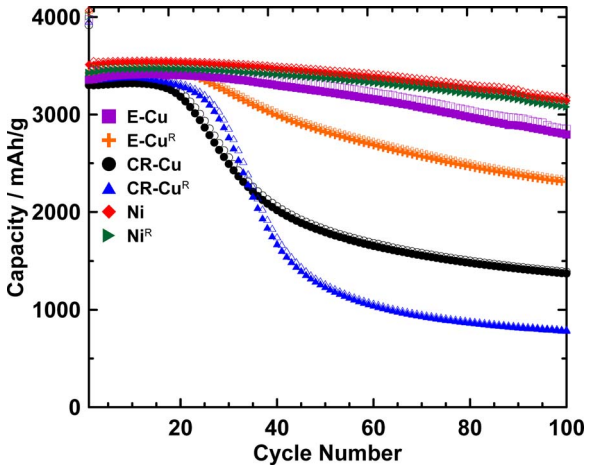

Figure 7. Cycling performance of a 275 nm Si thin film on different substrates. Opened and closed symbols represent lithiation and delithiation capacity, respectively.

to be poor, resulting in capacity fade. Roughening the Cu foil also results in fade, likely due to the Si film becoming detached at high radii of curvature apexes. It is well known that Si bonds strongly to Ni,[19] and, as a result, Ni is used as a bonding layer for Si wafer contacts in solar cells.[20,21] Good Si-Ni adhesion likely results in good cycling performance of the Si film on Ni foil, even when it is roughened.

Figure 8 shows the delithiation capacity, $Li_{15}Si_4$ peak area, and the change in average half-cycle potential (from the first cycle) plotted against cycle number for all the Si films on the different substrates shown in Figure 7. All films show fade commencing after about 15–20 cycles, although the fade is more severe for some films than for others. $Li_{15}Si_4$ formation is coincidental with fade in all cases. These results are consistent with the model proposed in Figure 6. However, cells experiencing larger capacity fade were not found to exhibit greater $Li_{15}Si_4$ formation as a fraction of total delithiation capacity. Instead, the films expected to have the best adhesion to Si (Ni, Ni^R, and E-Cu) cycle with a low fade rate despite the formation of $Li_{15}Si_4$. We suspect that the Si islands in these films that form after crack formation remain attached to the substrate by means of a small "patch" (as reported in Reference 22), which maintains electrical contact. Most of the area of such islands may be separated from the substrate and subject to low stress; therefore, they form considerable amounts of $Li_{15}Si_4$ at full delithiation. However, such islands can continue to cycle by virtue of their maintained electrical contact. In films on substrates with less adhesion, the ability to maintain electrical connection to the substrate via a small patch is reduced, and flake detachment and fade are accelerated.

The change in average half-cycle potential during cycling, also shown in Figure 8, provides further insight into the relationship between stress, $Li_{15}Si_4$ formation and capacity fade. For all films, the average delithiation potential decreases during initial cycles. This indicates that the tensile stress in the film becomes reduced every cycle, perhaps due to progressive crack formation. When fade and $Li_{15}Si_4$ formation start to occur the average delithiation voltage increases sharply. This is an artifact of the growth of the $Li_{15}Si_4$ peak at about 440 mV. During lithiation, the average voltage initially increases. This indicates that the compressive stress in the film becomes reduced every cycle, again likely due to progressive crack formation. The average lithiation voltage then reaches a plateau, until fade and $Li_{15}Si_4$ formation occurs. This is also where film detachment from the substrate commences, which should further reduce compressive stresses during lithiation. Indeed this is reflected by an increase in average lithiation voltage at the same moment when fade and $Li_{15}Si_4$ formation start, further reinforcing our model. During fade the average lithiation voltage increases to a plateau, except for the CR-Cu and CR-Cu^R foils. In these foils the average lithiation voltage decreases in later cycles,

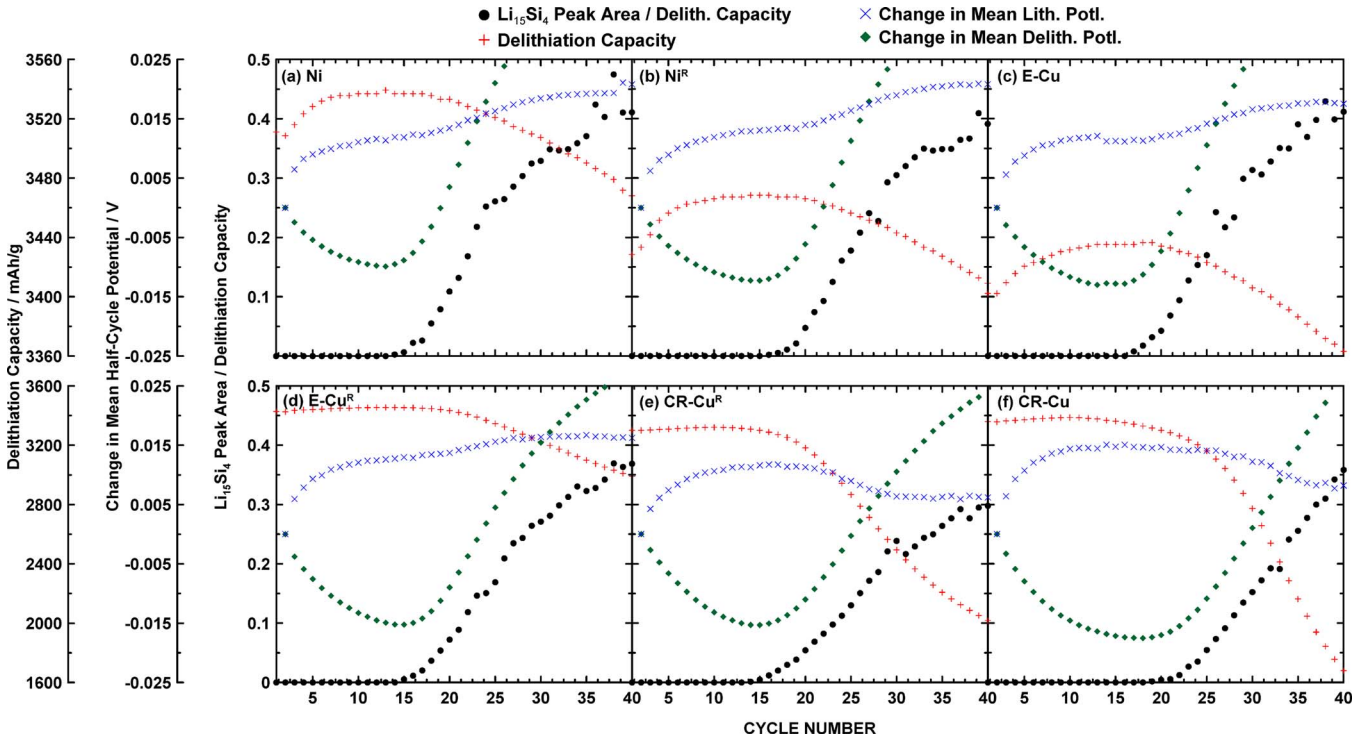

Figure 8. Delithiation capacity, relative $Li_{15}Si_4$ peak area, and change in mean half-cycle potential versus cycle number, for a 275 nm Si thin film sputtered onto substrates Ni, Ni^R, E-Cu, E-Cu^R, CR-Cu^R, and CR-Cu foil.

however this decrease in voltage is due to polarization. In these foils the fade is so severe that during later cycles the capacity is small, resulting in a significant increase in cycling rate, and the resulting polarization causes the lithiation voltage to decrease as observed.

To further understand the mechanism behind stress alleviation in Si thin films, the nature of the voltage shift needs to be clarified. For instance, stress could be reduced uniformly in the film, which would result in a uniform shift in differential capacity peaks. Alternatively, the stress could be relieved in an inhomogeneous manner, in which case one would expect the differential capacity peaks to both shift and become broadened as cycling progresses. In Figure 9, the full width at half maximum (FWHM) of cycles 2, 5, and 25 are plotted for the

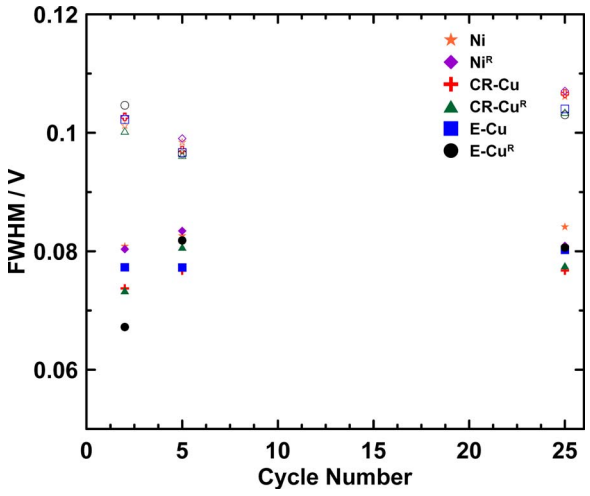

Figure 9. (a) Full width at half maximum (FWHM) of the lithiation peaks in the differential capacity curve for cycles 2, 5 and 25 for the sputtering run shown in Figure 7. The open and closed points represent the 200 and 90 mV lithiation peak positions, respectively.

electrodes used in Figure 8. The FWHM does not change appreciably during cycling. This indicates that stress is uniformly relieved in the Si film during cycling.

In order to determine if cycling rate had an effect on $Li_{15}Si_4$ formation, thin films were cycled at different cycling rates. In Figure 10a, the delithiation capacity and $Li_{15}Si_4$ peak area versus cycle number is shown for a 275 nm film sputtered onto E-Cu cycling at a C/50 rate. At this slow rate, $Li_{15}Si_4$ formation remains suppressed during early cycling and only emerges by cycle 17. Additionally, $Li_{15}Si_4$ formation is accompanied by capacity fade, which is the same behavior as observed in Figure 8 for Si films cycling at a C/2 rate. Figure 10b shows the differential capacity curves of the first three cycles of the same film cycling at a C/100 rate. Even at this extremely slow rate, no $Li_{15}Si_4$ is observed in early cycling. This result implies that the cycling rate may not play a large role in the suppression of $Li_{15}Si_4$ formation. Indeed, we have only been able to induce incomplete $Li_{15}Si_4$ formation in this film during the initial cycle by holding the film at a constant voltage of 5 mV for 100 hours. We speculate that after this length of time plastic flow may be reducing the internal stress, allowing some $Li_{15}Si_4$ phase to form.

So far in this study, the appearance of $Li_{15}Si_4$ has only been shown to be indicative of film disconnection from the substrate. A question remains as to whether the presence of $Li_{15}Si_4$ is detrimental to cycling. To determine this, 275 nm Si films sputtered onto CR-Cu and onto E-Cu were cycled to lower cutoff voltages of 5 mV (where $Li_{15}Si_4$ formation eventually occurs) and 25 mV (at which it was found $Li_{15}Si_4$ formation was avoided for this film). Cycling performance of these cells and their differential capacity are shown in Figures 11 and 12 for the CR-Cu and E-Cu foil substrates, respectively. In the case of the Si film on CR-Cu, fade occurs at about cycle 20 when $Li_{15}Si_4$ is formed. In contrast, fade commences at about cycle 50 when the lower voltage cutoff is raised to avoid $Li_{15}Si_4$ formation. It is difficult to believe that this significant difference in cycling performance is a result of the slightly greater cycled capacity for the film cycled to 5 mV. Instead, this is suggestive that $Li_{15}Si_4$ formation is detrimental to cycling. This has long been suspected to be the case, since 2-phase regions are thought to be detrimental to cycling.[23,24] This distinction

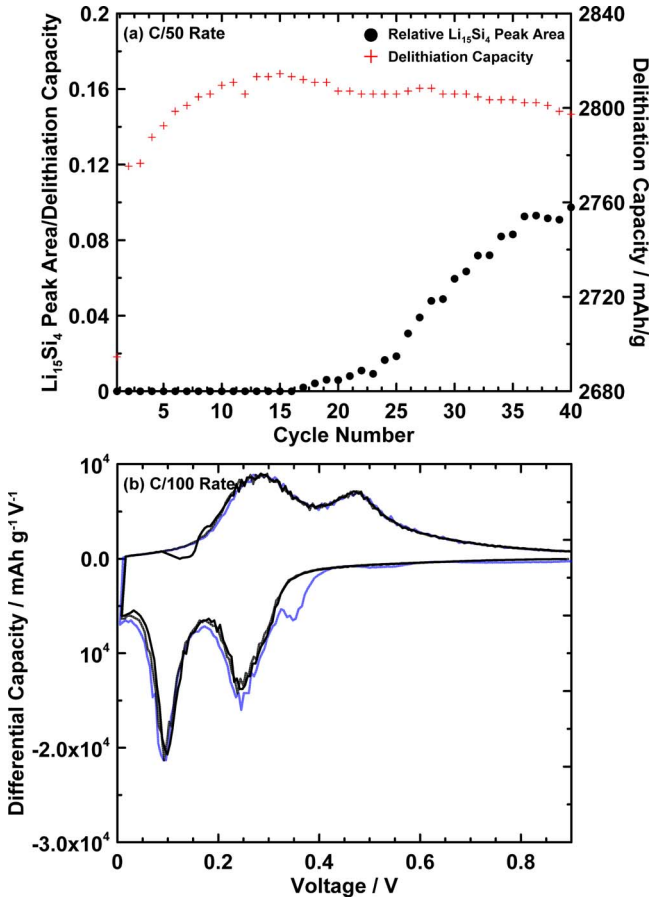

Figure 10. (a) Relative $Li_{15}Si_4$ peak area and delithiation capacity versus cycle number for a 275 nm film sputtered onto E-Cu cycling at C/50 rate. (b) Differential capacity curve of the first 3 cycles of the same film at C/100 rate, darker lines indicate later cycles.

is less clear for the film sputtered on E-Cu, shown in Figure 12. Less fade is indeed apparent for the cell with no $Li_{15}Si_4$ compared to the cell with $Li_{15}Si_4$ formation prior to cycle 60, however after cycle 60 both cells fade at the same rate. Film disconnection effects likely begin to dominate after later cycles. More measurements along these lines are required to confirm this result.

Conclusions

In this work, the mechanism of fade and $Li_{15}Si_4$ formation in Si thin films were examined. In contrast to past studies, $Li_{15}Si_4$ formation occurred in all films during cycling. We believe that previous studies terminated cycling prematurely, before $Li_{15}Si_4$ formation occurred. In all Si film thicknesses, for all substrates and cycling rates studied here, $Li_{15}Si_4$ formation was found to be closely correlated with capacity fade and also film detachment from the substrate. $Li_{15}Si_4$ also forms immediately when the Si thin film is removed from the substrate and is cycled in a composite coating. These observations strongly suggest that $Li_{15}Si_4$ suppression in thin films is due to stress induced from the presence of the substrate. As cycling progresses, the film progressively detaches from the substrate, resulting in fade and progressive $Li_{15}Si_4$ formation. These results were further confirmed by measurements of average half-cycle voltages, which were consistent with stress release during cycling and film detachment from the substrate. Lastly, it was found that $Li_{15}Si_4$ formation itself may have a detrimental effect on cycling, as has long been suspected.

These results suggest that the formation of $Li_{15}Si_4$ can be used as a sensitive indicator for Si regions that are weakly bound or disconnected from a substrate. If a peak from $Li_{15}Si_4$ is present in differential capacity during cycling to full lithiation, then the Si must be weakly bound to a substrate. If no $Li_{15}Si_4$ peaks are present in the differential capacity, then the Si must be strongly connected to a substrate. However, care must be taken when using this property that cells are cycled at a low rate, since high rate cycling can cause cell polarization, resulting in the suppression of $Li_{15}Si_4$ formation.[12]

These results have profound implications, not only for thin films, but also for Si alloys in general (including Si alloy particles). For instance in particles comprising an active Si phase and an inactive matrix phase, the presence of the inactive phase ought to induce

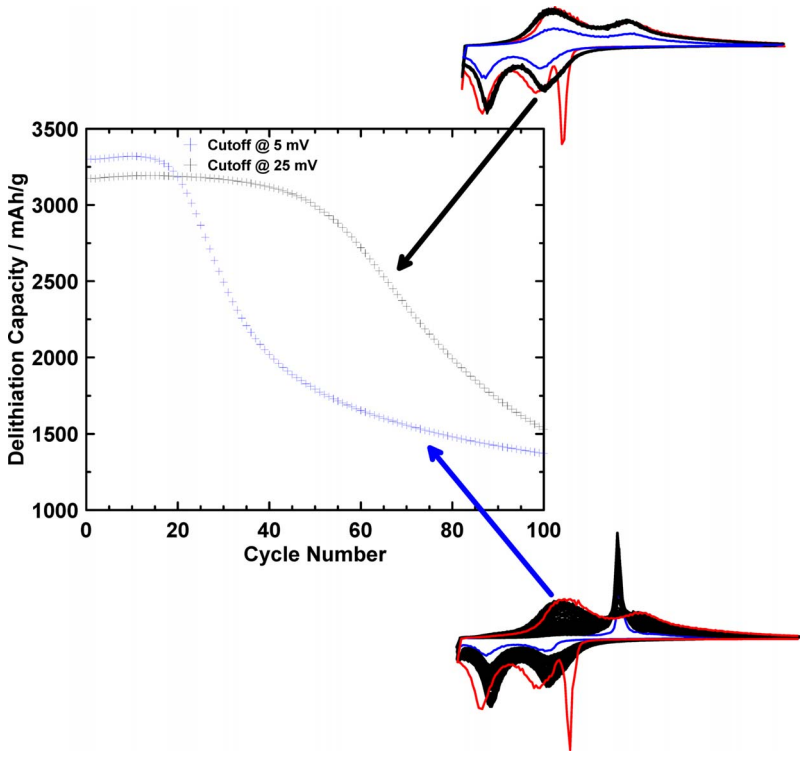

Figure 11. Delithiation capacity versus cycle number for 275 nm thick Si film sputtered onto CR-Cu cells with lower voltage cutoffs of 25 and 5 mV. Insets show the differential capacity curve for each cell where the first cycle is in red, cycles 10–50 are in black, and cycle 100 is in blue.

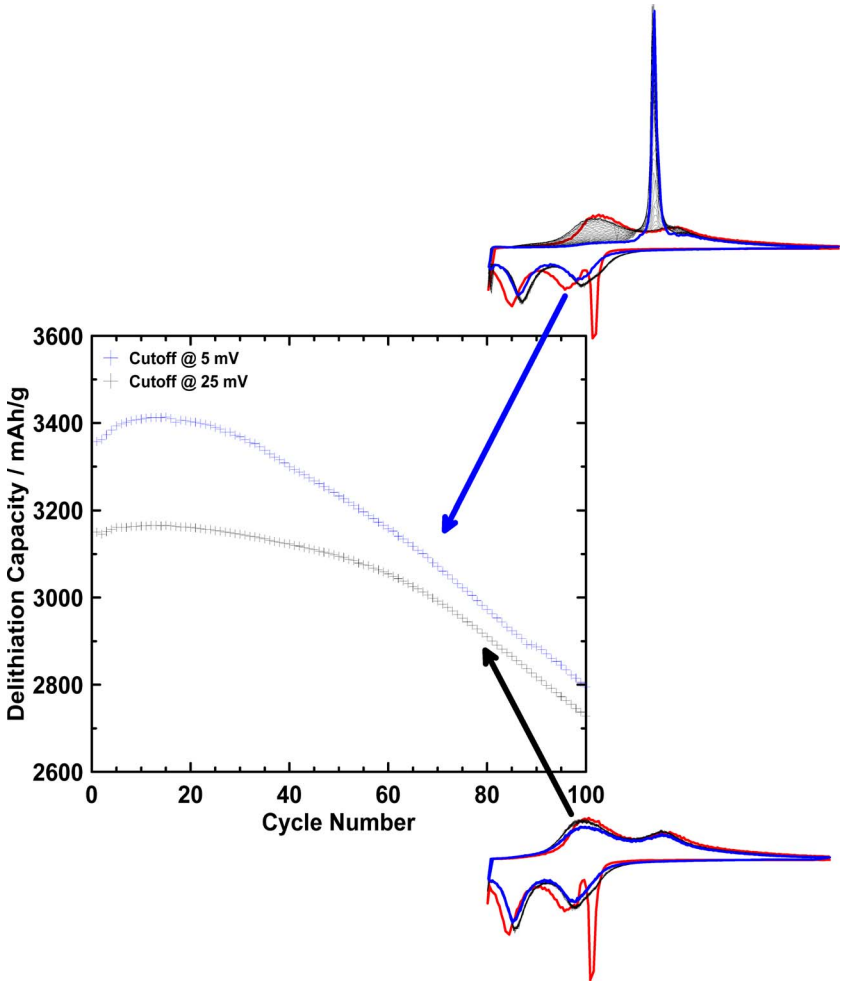

Figure 12. Delithiation capacity versus cycle number for a 275 nm thick Si film sputtered onto E-Cu cells with lower voltage cutoffs of 25 and 5 mV. Insets show the differential capacity curve for each cell where the first cycle is in red, cycles 10–50 are in black, and cycle 100 is in blue.

stress during the expansion/contraction of the active Si phase and suppress $Li_{15}Si_4$ formation, just as the substrate does in a Si thin film. We have found this to be exactly the case, as is demonstrated in Reference 25, and in other results which we will report in subsequent publications.

References

1. M. N. Obrovac and L. Christensen, *Electrochem. Solid-State Lett.*, **7**, A93 (2004).
2. K. Rhodes, N. Dudney, E. Lara-Curzio, and C. Daniel, *J. Electrochem. Soc.*, **157**, A1354 (2010).
3. X. H. Liu et al., *ACS Nano*, **6**, 1522 (2012).
4. M. T. McDowell et al., *Adv. Mater.*, **24**, 6034 (2012).
5. L.-F. Cui, R. Ruffo, C. K. Chan, H. Peng, and Y. Cui, *Nano Lett.*, **9**, 491 (2009)
6. B. Laïk et al., *Electrochim. Acta*, **53**, 5528 (2008).
7. S. W. Lee, M. T. McDowell, J. W. Choi, and Y. Cui, *Nano Lett.* (2011).
8. M. Green, E. Fielder, B. Scrosati, M. Wachtler, and J. S. Moreno, *Electrochem. Solid-State Lett.*, **6**, A75 (2003).
9. J. P. Maranchi, A. F. Hepp, and P. N. Kumta, *Electrochem. Solid-State Lett.*, **6**, A198 (2003).
10. J. P. Maranchi, A. F. Hepp, A. G. Evans, N. T. Nuhfer, and P. N. Kumta, *J. Electrochem. Soc.*, **153**, A1246 (2006).
11. Z. Du, R. A. Dunlap, and M. N. Obrovac, *J. Electrochem. Soc.*, **161**, A1698 (2014).
12. V. L. Chevrier et al., *J. Electrochem. Soc.*, **161**, A783 (2014).
13. I. Ryu, J. W. Choi, Y. Cui, and W. D. Nix, *J. Mech. Phys. Solids*, **59**, 1717 (2011).
14. T. D. Hatchard and J. R. Dahn, *J. Electrochem. Soc.*, **151**, A838 (2004).
15. V. A. Sethuraman, V. Srinivasan, A. F. Bower, and P. R. Guduru, *J. Electrochem. Soc.*, **157**, A1253 (2010).
16. V. A. Sethuraman, M. J. Chon, M. Shimshak, V. Srinivasan, and P. R. Guduru, *J. Power Sources*, **195**, 5062 (2010).
17. B. Yang et al., *J. Power Sources*, **204**, 168 (2012).
18. L. Y. Beaulieu, T. D. Hatchard, A. Bonakdarpour, M. D. Fleischauer, and J. R. Dahn, *J. Electrochem. Soc.*, **150**, A1457 (2003).
19. Y. Luo, *Comprehensive handbook of chemical bond energies*, CRC Press (2007).
20. K. Kholostov, L. Serenelli, M. Izzi, M. Tucci, and M. Balucani, *Mater. Sci. Eng. B*, **194**, 78 (2015).
21. J. Kanungo et al., *Semicond. Sci. Technol.*, **21**, 964 (2006).
22. L. Y. Beaulieu, K. W. Eberman, R. L. Turner, L. J. Krause, and J. R. Dahn, *Electrochem. Solid-State Lett.*, **4**, A137 (2001).
23. I. A Courtney, R. A. Dunlap, and J. R. Dahn, *Electrochim. Acta*, **45**, 51 (1999).
24. M. N. Obrovac and V. L. Chevrier, *Chem. Rev.*, **114**, 11444 (2014).
25. Z. Du, T. D. Hatchard, R. A. Dunlap, and M. N. Obrovac, *J. Electrochem. Soc.*, **162**, A1858 (2015).